DOI:10.16555/j.1006-8775.2015.02.002

Article ID: 1006-8775(2015) 02-0111-10

SEA SURFACE TEMPERATURE RESPONSE TO TYPHOON MORAKOT (2009) AND ITS INFLUENCE

LAI Qiao-zhen (赖巧珍)[1], WU Li-guang (吴立广)[2], SHIE Chung-lin (谢钟灵)[3]
(1. Longyan Meteorological Office of Fujian Province, Longyan 364000 China; 2. Nanjing University of Information Science & Technology/Key Laboratory of Meteorological Disaster of Ministry of Education, Nanjing 210044 China; 3. UMBC/Goddard Earth and Sciences Technology Center, NASA Goddard Flight Center, Greenbelt, Maryland, USA)

Abstract: While previous studies indicate that typhoons can decrease sea surface temperature (SST) along their tracks, a few studies suggest that the cooling patterns in coastal areas are different from those in the open sea. However, little is known about how the induced cooling coupled with the complex ocean circulation in the coastal areas can affect tropical cyclone track and intensity. The sea surface responses to the land falling process of Typhoon Morakot (2009) are examined observationally and its influences on the activity of the typhoon are numerically simulated with the WRF model. The present study shows that the maximum SST cooling associated with Morakot occurred on the left-hand side of the typhoon track during its landfall. Numerical simulations show that, together with the SST gradients associated with the coastal upwelling and mesoscale oceanic vortices, the resulting SST cooling can cause significant difference in the typhoon track, comparable to the current 24-hour track forecasting error. It is strongly suggested that it is essential to include the non-uniform SST distribution in the coastal areas for further improvement in typhoon track forecast.

Key words: sea surface temperature; typhoon; ocean response; typhoon track forecast
CLC number: P444 **Document code:** A

1 INTRODUCTION

The response of the ocean to tropical cyclone (TC) forcing is of considerable scientific and practical importance (Price[1]). A TC can result in a cooling of the mixed layer through entrainment and upwelling. According to buoy observation and numerical simulation, the TC-induced sea surface temperature (SST) cooling ranges from 1-6℃ over the open sea (Lin et al.[2]; Shang et al.[3]). With the improvement of observational techniques, significant cooling has once been observed. The SST cooling depends on the strength and translation speed of a TC and its marine environment. In general, the slower the TC moves, the larger the sea surface cooling is (Zheng et al.[4]; Brand[5]).

It is well recognized in many previous studies that the SST cooling is more towards the right of the storm track, because of the dominant wind stress forcing there on the open ocean. However, some recent studies discovered that this is true only in the open ocean but not for the near-coastal waters. As a cyclone translates over the coastal waters, the impedance of the coastline to the circulation and strong cold eddy shift the region of maximum surface cooling to the left of the cyclone track (Yang and Tang[8]; Mahapatra et al.[9]).

Almost all studies agree that the TC induces the SST to drop, leading to a negative feedback. The cooling of the sea surface near the core of the storm results in the reduction in the total heat flux and energy production into the atmosphere, tending to dampen the storm intensity, but there is a big controversy over whether SST cooling can influence the TC track and how. Comparison of coupled model experiments (by considering SST drop caused by TC) and fixed SST experiments obtained different results. Some find the SST cooling causes a westward-moving (eastward-moving) TC far southward (northward), while the others show that the migration of a TC is very sensitive to the change of the periphery tangential wind profile, and the SST anomalies reduce the tangential airflow, making TCs turn to the north (south). Some researchers argued that the SST cooling has little effect on the TC track, because the change of tangential airflow caused by the SST cooling is too small to affect TC movement (Ben der and Ginis[14]; Zhu et al.[15]). Wu et al.[16] respectively considered the role of the symmetric and asymmetric part of the SST cooling and came to a similar conclusion. Although the proportion of the symmetric part of the SST cooling is small, it obviously weakens TC intensity and external forces, thereby increasing the northern component of β -drift, and resulting in the deviation to the polar region of westward-moving TCs. On the contrary, the asymmetrical part of the SST cooling enhances the adiabatic heating to the south of a west-

Received 2014-01-02; **Revised** 2015-03-06; **Accepted** 2015-04-15
Foundation item: National Key Technology Research and Development Program of China (2009CB421503); New Recruitment Graduate Project of the Fujian Province Meteorological Bureau (2012G01)
Biography: LAI Qiao-zhen, Ph. D., associate researcher, primarily undertaking research on tropical cyclones.
Corresponding author: WU Li-guang, e-mail: liguang@nuist.edu.cn

ward-moving TC, tending to shift it southward. Because the two effects cancel each other, the impact of SST cooling on TC track is very small.

It is noted that the above studies are mainly on air-sea interaction in the open sea, while few concerns are in the near-coast waters, particularly in the surrounding waters of the Taiwan Strait. However, enhanced awareness in this aspect is of great significance for further improvement of the TC track forecast and strengthening of disaster prevention in the coastal cities. Therefore, based on satellite SST data, we analyze the SST response to Typhoon Morakot (2009) in the near-coast waters with cold eddies, Kuroshio, and upwelling and then examine the influence of SST cooling on TC track, and the extent of the effect based on numerical simulation.

2 DATA

We used the SST data from the National Climatic Data Center (NCDC) to analyze the SST response to TC activity. The daily average SSTs with relatively high resolution (0.25°×0.25°) are composed from the Advanced Very High Resolution Radiometer (AVHRR) and Advanced Microwave Sounding Radiometer for the Earth Observing System (AMSR-E). In high latitudes, this AVHRR & AMSR-E SST data is better to reflect the gradient distribution of SST. In strong precipitation areas, however, the error increases (Richard et al.[17]).

In order to understand the distribution of mesoscale eddies, the sea surface height anomalous (SSHA) data from the Center National D'Etudes Spatiales (CNES) was used. Its spatial resolution is 1/3°, and the time-gap is 7 days from January 1998 to December 2010 with the measuring error of 2-3 cm (Blanc et al.[18]) .

The Goddard Satellite-based Surface Turbulent Fluxes (GSSTF2, version 2) model data in the NASA database provide the sea surface heat flux and 2-m wind speed (Shie[18]). The spatial resolution of the daily and monthly average gridded global model data is 1°, and its time span is from July 1987 to December 2008. Turbulent flux was computed as bulk flux. Compared with the other turbulent flux, such as Hamburg Ocean-Atmosphere Parameters and Fluxes (HOAPS) satellite data, NCEP-NCAR re-analysis flux data and the flux data in the Comprehensive Ocean-Atmosphere Data Set (COADS), they will more truly reflect the ocean disturbance characteristics of flux. Because of the lack of data in 1987, we have only used 21-year data (from January 1988 to December 2008) to describe the offshore environment.

The initial and boundary conditions of the WRF model are derived from National Centers for Environmental Prediction (NCEP) model analyses with 26 mandatory layers (1 000-10 hPa), including SST, sea level pressure, geopotential height, temperature, relative humidity, wind and other factors.

The TC data of this study are obtained from the Japan Meteorological Agency (JMA), including the TC location and intensity in the northern West Pacific basin (northern West Pacific and South China Sea) at 6-h intervals.

3 FEATURES OF THE COASTAL SEA

The ocean current around Taiwan Island is complex, especially due to the Kuroshio Current (KC), a current in the western boundary of the Pacific. Fig.1a marks the approximate average position of KC in August. The SST contours extend to Yellow Sea, Korea Strait and the Sea of Japan, manifesting the existence of KC.

Figure 1b gives the spatial distribution of the sea surface heat fluxes, which shows gradients in both longitudinal and latitudinal direction. Due to the influence of the coastal upwelling, 2-m-high wind speed over these areas is smaller than the wind over offshore sea. Therefore, the region of the smallest heat flux lies in the upwelling area around Dongshan Island. The region of maximum heat flux along the mid-latitude Kuroshio is associated with high SST and strong westerly wind. The distribution pattern of SST (Fig.1a) is very similar to that of the heat flux. The longitudinal gradient is caused by the longitudinal variation of solar radiation, while the latitudinal gradient is mainly due to the existence of KC, coastal upwelling, and cold eddies on the near-coast waters.

The spatial scale of ocean mesoscale eddies is from 50 to 500 km, and the maximum vertical dimension up to 5 km, being of a few days to a few months in lifespan. These eddies can be divided into the cyclonic and anticyclonic eddies with high energy. Surface water of the cyclonic vortex diverges due to the Coriolis force, which reduces the Ekman pumping effect. Therefore, cyclonic eddies correspond with the lower SST than the surrounding area. The SST on the KC is about 30℃ in summer and higher than 20℃ in winter, so the ocean surface usually exhibits consistently warm SST. Therefore, it is difficult to use SST data to identify these eddies. Satellite SSHA measurements have proven to be very effective in identifying ocean eddies and quantifying eddy characteristics since it has the high accuracy of 2-3 cm for every 7-d cycle. Therefore, this study uses the negative value area of sea-surface height anomaly to characterize the cold eddies around Taiwan Island. Fig.2 is the SSHA distribution in August. We can see that there are some cold and warm eddies in the near-coast waters.

Obviously, the near-coast marine environment is complex. There are not only KC and mesoscale cold/warm eddies, but also the gradient of SST and heat flux, which would affect the energy production into the atmosphere and the air-sea interaction.

4 ACTIVITY OF TYPHOON MORAKOT (2009)

Typhoon Morakot is the most powerful TC among

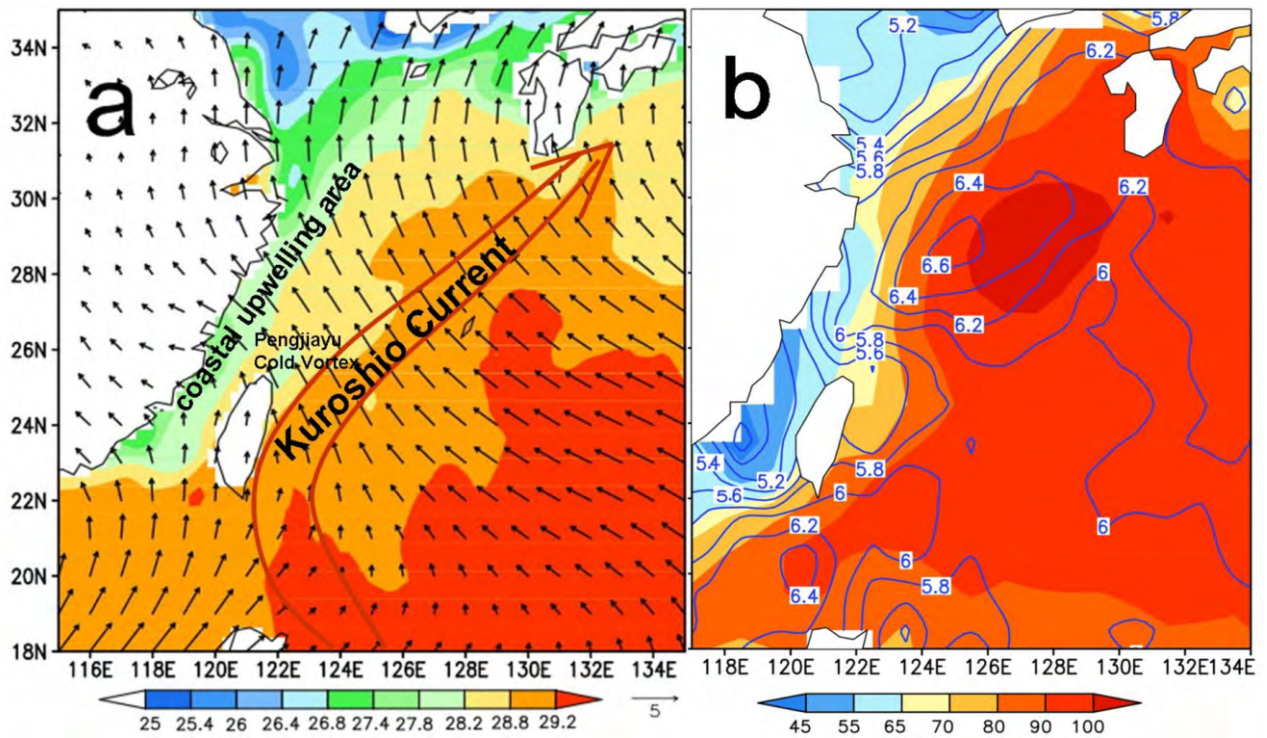

Figure 1. Coastal marine environment. (a) Monthly average SST and wind field on 850 hPa in August from 2002 to 2009. The shadow is for SST and the arrow for the wind vector; (b) monthly average sea surface heat flux (shadow) and 2-m wind speed (isoclines) in August from 1988 to 2008. SST unit: ℃, wind speed unit: m/s; contour interval is 0.2 m/s.

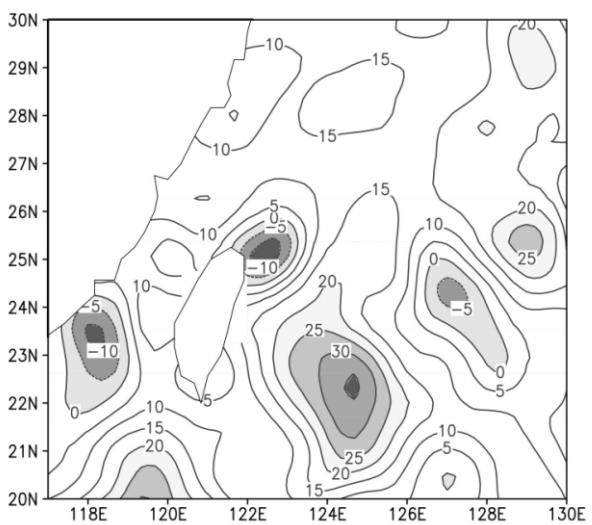

Figure 2. SSHA on August 2009(cm). Shadows are anomalies less than 0 cm or greater than 20 cm; contour interval is 5 cm.

the TCs affecting China in 2009, which formed on 3 August, strengthened to a TC on 5 August, and made the first landfall on Taiwan Island with maximum wind up to 40 m/s on 7 August. When the TC made the second landfall in Fujian province, its maximum wind still reached 33 m/s. On 9 August, the TC weakened into a strong tropical storm and became a depression in the evening of 11 August.

Anthes and Chang[21] showed that, if the time of TC activity on a warm area is less than 12 h, SST has little impact on TC activity. However, Morakot maintained more than 35 h across the Taiwan Straits and provided enough time to the interaction between the TC and ocean, so this is an excellent case for studying the air-sea interaction in the presence of TCs.

Figure 3 shows the TC track. Before its first landfall on Taiwan Island, Morakot traveled westward and then headed northwestward to the island. Morakot shifted northward again until it made the second landfall on Fujian province. Some studies have focused on the binary interaction between Morakot and Goni and the topographic effect on the track, but little is known about the impact of the non-uniform distribution of the coastal SST and SST cooling induced by the TC.

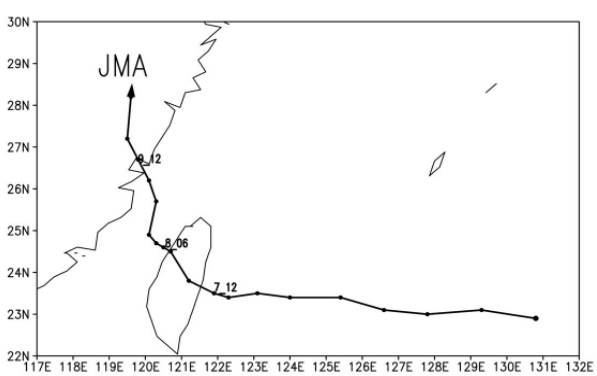

Figure 3. Track of Morakot form JMA's best-track data. The storm position is denoted every 6 h.

5 COASTAL OCEAN RESPONSE TO MORAKOT

The SST significantly dropped after Morakot passed and eventually the maximum SST cooled up to -3.5℃. There are two methods for calculating SST cooling in the previous studies. In the early stage, Price et al.[1] proposed that SST variations are the difference between the time before and after TC passed ($\triangle SST=SST_{t+1}-SST_{t-1}$, t for the time when the TC reaches the study area). Recently, they took the SST for anytime of TC passage minus the SST before TC formed. Because the SST response lags the TC activity, we use another method in this study. The specific algorithm is $\triangle SST=SST_p-SST_b$. Here b is the date of TC formation and p represents the time (in day) during the TC activity. Fig.4 shows the SST cooling associated with Morakot.

On the open sea, the maximum SST decrease associated with Morakot occurred to the right of the storm track, while the ocean response on the left area of TC track is stronger than the right area as the TC advanced for the landfall (Fig.4a, SST cooling up to 1.5℃ on the left, but only 0.5-1℃ on the right near 123°E). On 8-9 August, Morakot passed through the Taiwan Strait, causing the maximum SST decrease which was also located to the left, rather than to the right (Fig.4b). As one of the possible reasons, when the TC approached the eastern coast, the winds along the front edge of the TC are northerly and thus the net Ekman transport would be towards the coast. However, as the TC approached the coast further, onshore transport continues to its right while offshore transport develops to the left. The offshore transport and upwelling causes more SST cooling to the left. Thus, serving as an obstacle to Ekman transport and causing the piling up of waters, the coast is responsible for the transformation of the region of maximum sea surface cooling from right to left during the time of landfall (Mahapatra et al.[9]). In addition, other reasons may cause the SST to cool.

Figure 5a shows the SSHA distribution on 5 August. There is a small negative area that indicates a cold eddy to the southeast of Taiwan Island. After the TC passed, the cold eddy was further strengthened (Fig.5b), enhancing the sucking effect caused by Morakot. Therefore, the cold eddy effect to the left of the path makes the SST response more significant. Comparing the sea-level anomalies before and after the Morakot passage (Fig.5) indicates that Morakot not only caused the cold wake, but also strengthened the cold eddies near the path. The same conclusion came from Yang and Tang [8], in which TC activity will strengthen the cold eddies existing in the upper sea layer and cold eddies play an important role in the magnitude and distribution of SST decrease caused by TCs.

In summary, due to the complex coastal marine environment, the coastal SST response to Morakot is different from that of the open sea. The sea surface response to the left of the TC track is more obvious than to the right, and the region of maximum SST cooling associated with Morakot also occurred to the left of the TC track during the time of landfall with the coastline and cold eddy effects.

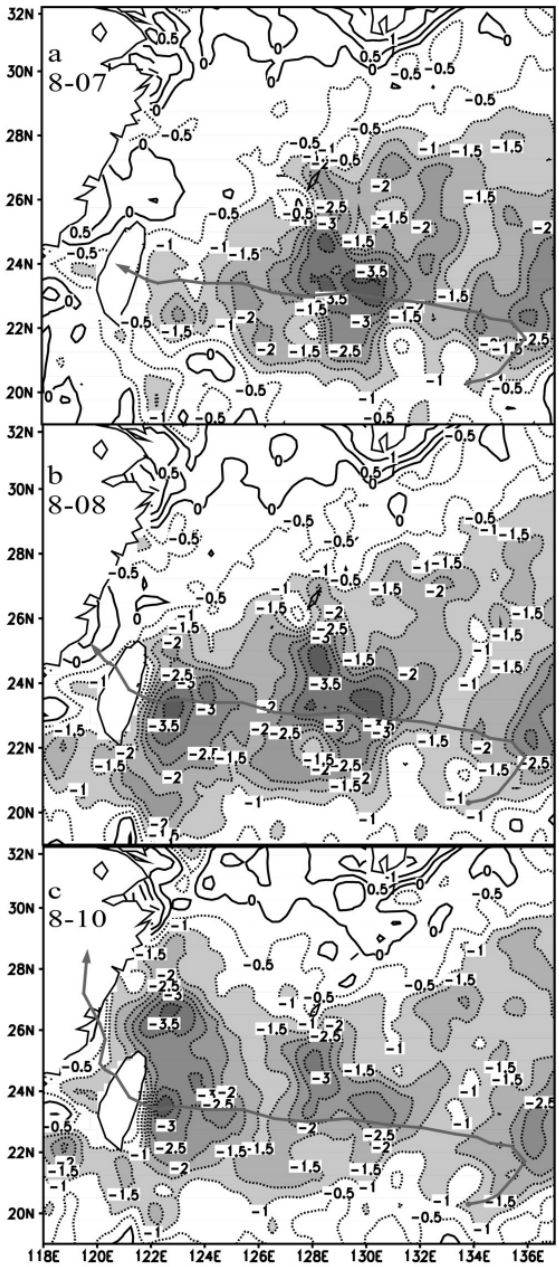

Figure 4. SST cooling caused by Morakot (△SST). △SST= SSTp-SST8/3, and 8/3 is on 3 August; p represents some day during TC activity; (a) 7 August; (b) 8 August; (c) 10 August. Shadows are SST cooling greater than 1℃; contour interval is -0.5℃; TC track is shown in bold line.

6 NUMERICAL SIMULATION

6.1 *Experiment design*

The WRF model has been extensively used in the simulation of TCs. The simulation of Typhoon Chanchu by Liu et al.[20] showed that the introduction of the daily observations of SST can significantly improve the accu-

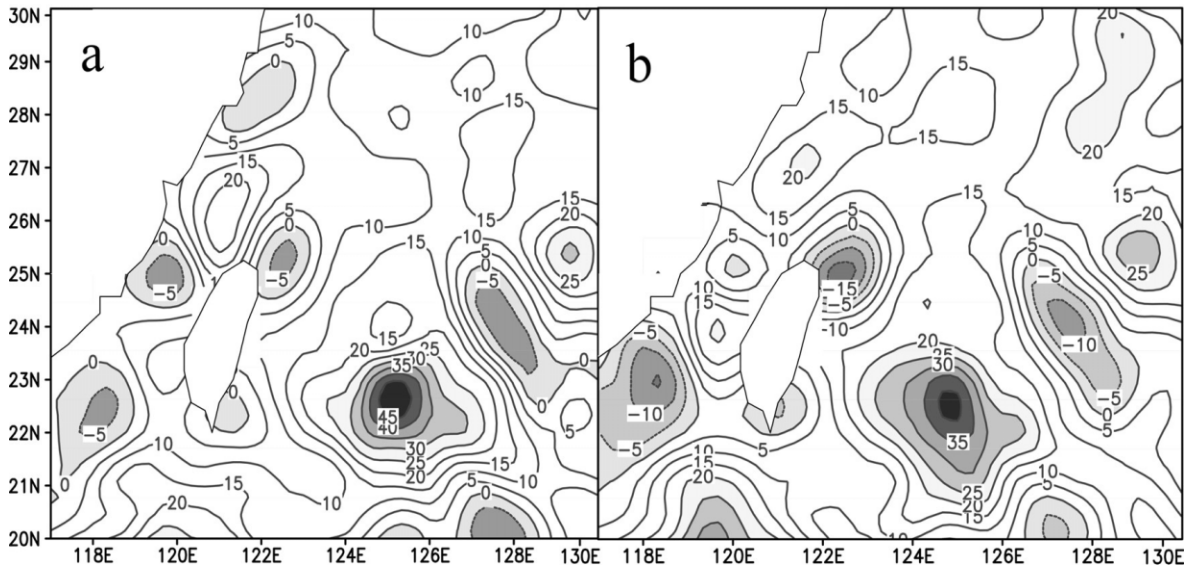

Figure 5. SSHA (cm). (a) 5 August; (b) 12 August. Shadows are anomalies less than 0 cm or greater than 25 cm; contour interval is 5 cm.

racy of simulated TC intensity.

The model domain is centered at 125°E, 25°N and its initial and boundary conditions are derived from the NCEP reanalysis. A triple two-way nesting grid system is used, in which the third mesh moves with the TC. The horizontal resolution of the grids are 27 km, 9 km, and 3 km, respectively, consisting of 200×200, 300×300, and 180× 180 grid points. The integration time is from 1200 UTC 5 August to 0000 UTC 10 August 2009. The first-grid uses a shallow convection Kain-Fritsch (new Eta) scheme while the second and third-grid do not use it.

To know the impacts of SST on TC track and intensity, this paper designed five experiments (Table 1). The SST field of the control experiment (CTL experiment) comes from the relatively even NCEP-SST data, which reflect the meridional SST gradient, but fail to reflect the complexity of coastal SST distribution as well as the SST cooling caused by the TC (Fig.6a & b). The constant SST of the experiment (05AVE experiment) is 29.2℃ on 5 August within the area of 20° to 30° N, 116° to 132° E. This test does not consider the impact of SST decrease and SST gradients on TCs. In the Satellite SST experiment (SATE-SST experiment) SST from the AVHRR/AMSR-E satellite is updated on a daily basis. Because the SST distribution is the closest to the reality and changes with the development of the typhoon (Fig.6c & d), the test is expected to get better simulation results. The differences of SATE-SST and CTL tests are shown in two ways: SST cooling and coastal complex SST gradient. In order to understand individual influences of these two factors, COLD-EDDY and STRAIT sensitivity experiments are designed. The SST field in the Cold Eddy experiment is updated every 6 h based on the Control test, but the SST to the east of Taiwan Island is replaced with the AVHRR/AMSR-E satellite SST to indicate the SST cooling (Fig.6e & f). In the Strait experiment, the SST in the Taiwan Strait is replaced (Fig.6g & h) to discuss the impact of the coastal uneven SST distribution compared with the 05AVE test. The SST field in the COLD-EDDY and STRAIT tests consists of two parts,

Table 1. Design of the experiments.

Model	Experiment scheme
CTL	Control experiment, SST field updates every 6 h with the NCEP SST data from 1200 UTC 5 August to 0000 UTC 10 August
05AVE	fixed SST experiment, SST does not vary with time with the area average satellite SST (29.2℃) on 5 August within the area of 20° to 30°N, 116° to 132°E
SATE-SST	Satellite SST experiment, SST field updates every 6 h with AVHRR/AMSR-E satellite daily SST (SST for four times on the same day is the same)
COLD-EDDY	Cold Eddy experiment, SST field updates every 6 h based on the Control experiment but replaces the SST to the east of Taiwan (121° to 132°E) by AVHRR/AMSR-E satellite SST
STRAIT	Strait experiment, SST field updates every 6 h based on the Control experiment but replaces the SST on the Taiwan Strait (116° to 121°E) by AVHRR/AMSR-E satellite SST

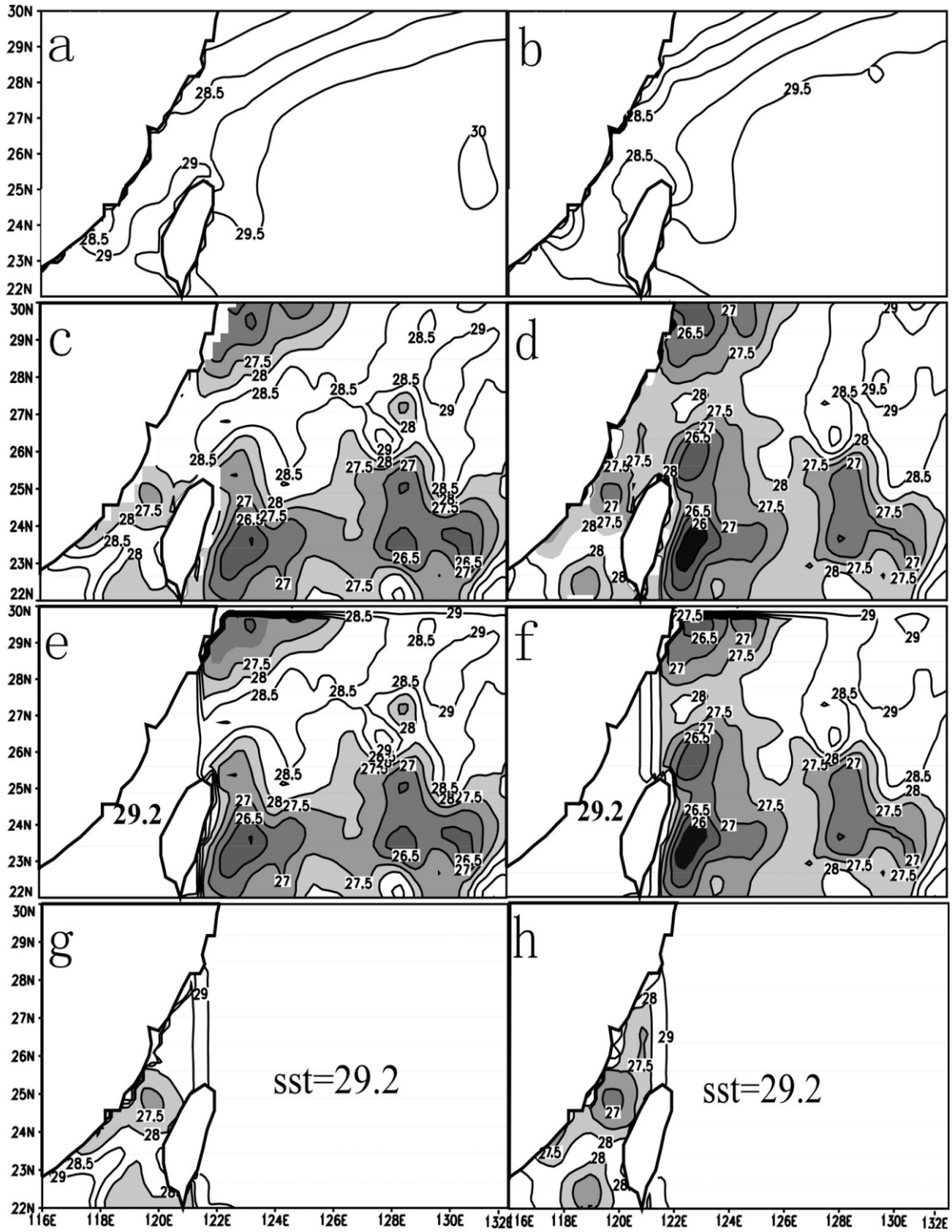

Figure 6. Model SST on 8 and 9 August (℃). (a, b) SST of CTL experiment; (c, d) SST of SATE-SST experiment; (e, f) SST of COLD-EDDY experiment; (g, h) SST of STRAIT experiment.

so we make the SST begin to increase generally at a rate of 0.2℃ at the junction area between these two different SST fields to reduce the impact of the dense gradient.

6.2 *TC track analysis*

6.2.1 TRACK SIMULATION

Figure 7 gives the observed track of Morakot from the JMA best-track data and three model tracks. In the open sea, these tracks differ little but all move more northward than the best track. When crossing the Taiwan Island, all simulations show the track change. However, on the coastal area, the track in SATE-SST experiment is closer to the best track than the control experiment. After landing, tracks are not well simulated.

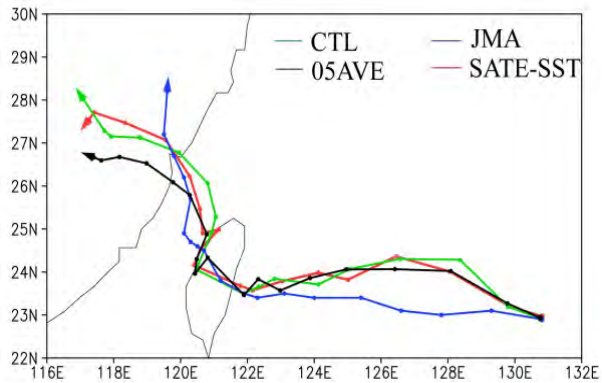

Figure 7. The observed track of Morakot and three model tracks. The storm position is denoted every 6 h.

For the TC landing point, the model results are accurate except the 05AVE experiment, and all fail to simulate the landing time. Comparing the track of 05AVE experiment with SATE-SST experiment indicates that the differences of tracks are small in the open sea but more obvious in the near-coast waters. Does this indicate that the effect of the coastal SST gradient on TC track is more obvious than SST drop in the open sea?

To understand the impact of the cold wake caused by TCs and coastal non-uniformly distributed SST on TC track, the results of three group sensitivity experiments (COLD-EDDY experiment, STRAIT experiment, and 05AVE experiment) are compared. For the COLD-EDDY experiment and 05AVE experiment, the model results discuss if the SST cooling could affect the track, while the other contrast between the STRAIT and 05AVE experiment is to examine the role of uneven distribution of SST on the Taiwan Strait.

6.2.2 IMPACT OF THE COLD WAKE ON TC TRACK

Figure 8a shows the differences in TC tracks between the 05AVE and COLD-EDDY experiment and its quadratic trend. Because the system error increases with the integration time, for a more accurate analysis of the impact of SST, we subtract the trend value from the initial difference and the result is shown in Fig.8b. Large differences in these two tracks appear from 1200 UTC 7 August to 0000 UTC 8 August, and reach the maximum at 1800 UTC 7 August when the TC crosses the Taiwan Island. The tracks difference is small before TC landing or after TC crossing over the Taiwan Island so the obvious difference may be caused by the terrain, but not induced by the SST cooling. This result also confirms the conclusion given by Wu et al. [16] based on a coupled hurricane-ocean model that the SST cooling reduces TC strength clearly while it has little effect on TC track.

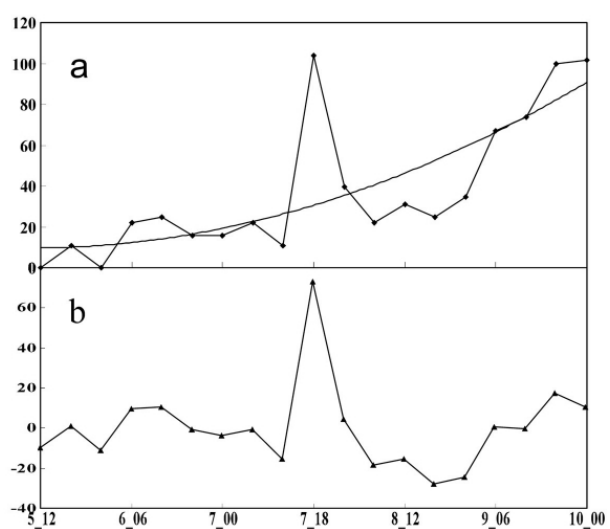

Figure 8. The track difference between COLD-EDDY and 05AVE experiment (km). (a) track difference and its quadratic trend; (b) track difference after subtracting the trend value.

6.2.3 IMPACT OF THE COASTAL SST ON TC TRACK

The SST field in the STRAIT experiment is the same as in the 05AVE experiment to the east of Taiwan Island, so the difference in TC tracks is not large. When TC reaches the Taiwan Strait, due to the different SST, the track differences become clear (Fig.9). The average difference is only 22 km before the TC reaches the Taiwan Strait, however, in the Taiwan Strait, the mean difference is up to 73 km, and the maximum difference is about 134 km at 0000 UTC 9 August. This deviation matches the current 24-h track forecasting error of China Meteorological Administration at 2009 [21], therefore the effect of coastal uneven SST on TCs cannot be neglig-

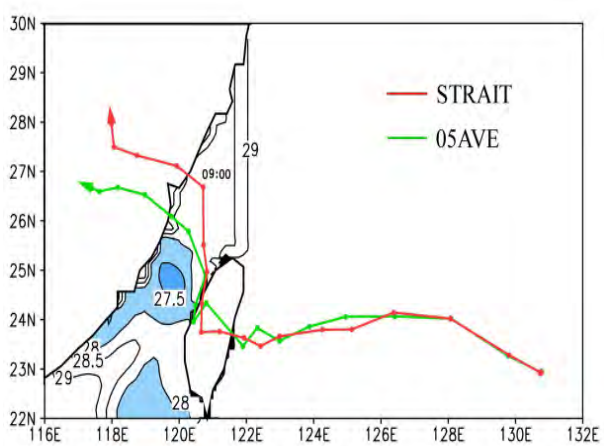

Figure 9. TC tracks of STRAIT and 05AVE experiment and SST on the Taiwan Strait of STRAIT experiment (℃).

ligible.

Figure 10 shows the distribution of simulated precipitation rates. The TC precipitation becomes more asymmetric under the non-uniform SST field in the Taiwan Strait. Wu et al. [24] suggested that a wavenumber-one diabatic heating could move TC to the region with the maximum diabatic heating. Chan [25] also pointed out that to the east and north of the TC center there is a strong vorticity area which corresponds to the vapor convection area on the middle and lower levels, result-

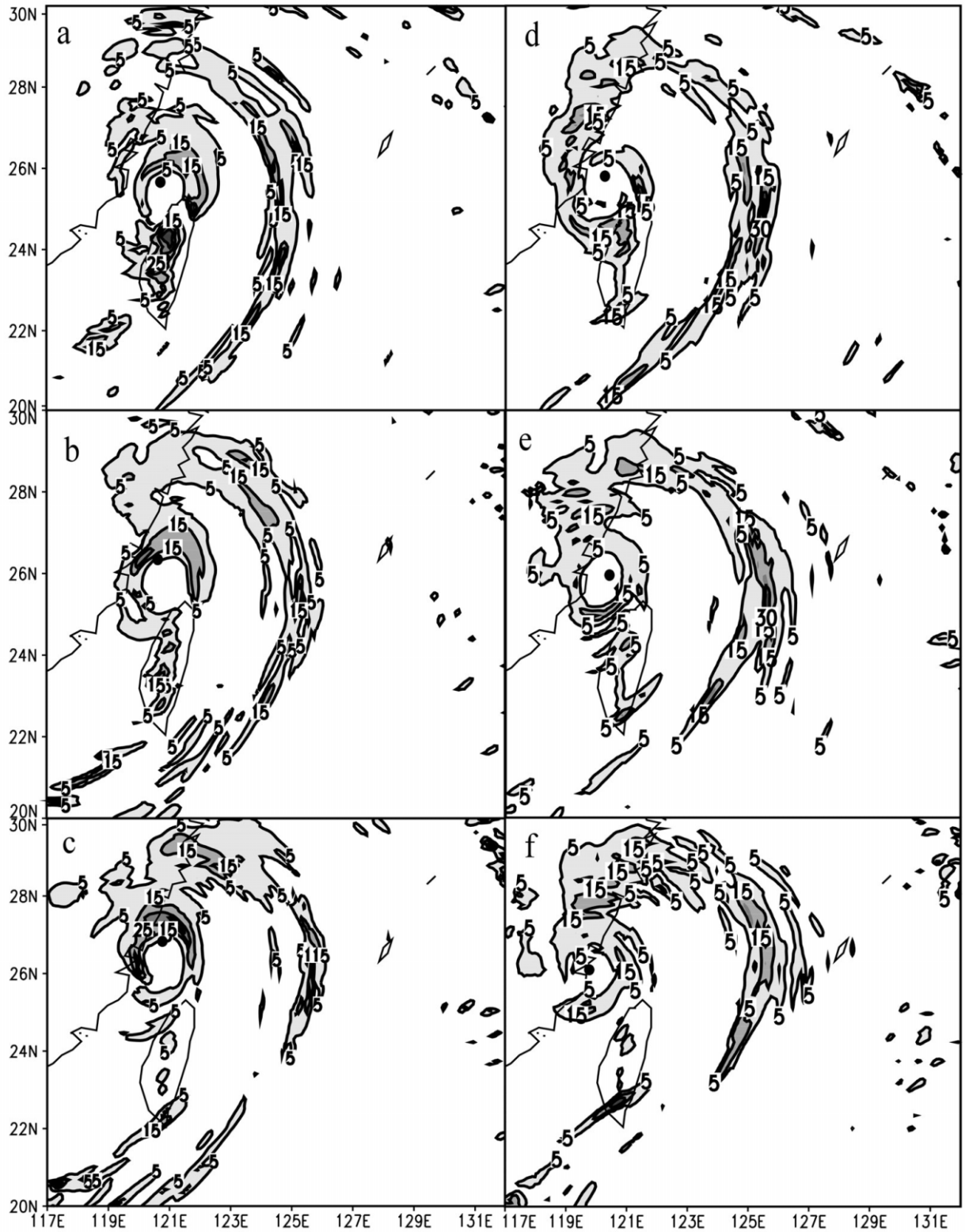

Figure 10. The distribution of simulated precipitation rate every 3 h (mm/h). a, b and c are the precipitation rates of STRAIT experiment at 1800 UTC 8 August, 2100 UTC and 0000 UTC 9 August; d, e and f are for the 05AVE experiment. Shadows are precipitation rates greater than 5 mm/h; contour interval is 10 mm/h.

ing in a large northward positive vorticity advection. As a result, the TC exhibits a northward motion component. At the STRAIT experiment, because the SST to the north of Taiwan Strait is higher than to the south, the enhanced diabatic heating is on the northern side of TC, tending to shift the TC northward. For the 05AVE experiment, however, for the uniform SST, the TC rainfall is more even and the northward deflection is small.

The above analysis suggests that the SST fall caused by TCs in the open sea has little influence on the track, but the SST gradient on the coastal area induces more asymmetry in the TC and causes it to move toward the maximum diabatic heating area.

7 CONCLUSIONS

The marine environment around Taiwan Strait is complex due to the presence of the KC, upwelling, ocean mesoscale eddies, as well as the gradients of heat flux and SST. For this reason, the SST response to Morakot in the near-coast waters is different from that over the open sea. The SST cooling from AVHRR / AMSR-E satellite SST data shows that the maximum is up to 3.5℃ in the open sea, mainly to the right side of the TC track, which is consistent with previous studies. In the near-coast waters, the response to the left of TC track is stronger, and the region of maximum SST cooling shifts to the left side of the track, due to the effect of the coastline and the cold eddies.

Complex near-coast marine environment not only makes the SST response different from that in the open sea, but also affects the movement of the TC. We use the WRF model to simulate the influences of the SST variations. Numerical simulations show that, the TC track of the SATE-SST experiment is the closest to the observation. The SST cooling forced by Morakot in the open sea has little impact on TC track but more impact on the near-coast waters together with the SST gradients. Non-uniform distribution of SST strengthens the asymmetry of the TC structure, tending to shift the TC northward (towards the enhanced diabatic heating area). The track difference between the STRAIT experiment and the 05AVE experiment is comparable to the current 24-h track forecasting error.

In brief, the marine environment of the near-coast waters is complex. The SST exhibits a large gradient, which makes the sea surface response to a TC different from the open sea. Uneven distributions of SST can change TC structure and affect TC movement. It has been shown that it is essential to include the non-uniform SST distribution in the coastal areas for further improvement in TC track forecast.

REFERENCES:

[1] PRICE J F. Upper ocean response to a hurri cane [J]. J Phys Oceanogr, 1981, 11(1): 153-175.

[2] LIN I I, LINW T, WU C. New evidence for enhanced ocean primary production triggered by tropical cyclone [J]. Geophys Res Lett, 2003, 30, 1718, doi: 10.1029/2003 GL017141.

[3] SHANG S, LI L, SUN F. Changes of temperature and bio-optical properties in the South China Sea in response to Typhoon Lingling, 2001 [J]. Geophys Res Lett, 2008, 35, L10602, doi: 10.1029/2008GL033502.

[4] ZHENG Z W, HO C R, KUO N J. Importance of pre-existing oceanic conditions to upper ocean response induced by Super Typhoon Hai-Tang [J]. Geophys Res Lett, 2008, 35, L20603, doi: 10.1029/2008GL035 524.

[5] BRAND S. The effects on tropical cyclone of cooler surface waters due to upwelling and mixing pro duced by a prior tropical cyclone [J]. J Appl Meteorol, 1971, 15(1): 909-919.

[6] BLACK P G. Ocean temperature changes induced by tropical cyclones [D]. The Pennsylvania State University, 1983: 278 pp.

[7] WADA A. Numerical simulations of sea surface cooling by a mixed layer model during the passage of Typhoon Rex [J]. J Oceanogr, 2005, 61(1): 41-57.

[8] YANG Xiao-xia, TANG Dan-ling. Location of sea surface temperature cooling induced by typhoon in the South China Sea [J]. J Trop Meteorol, 2010, 29(4): 26-31 (in Chinese).

[9] MAHAPATRA D K, RAO A D, BABU S V, et al. Influence of coast line on Upper Ocean's response to the tropical cyclone [J]. Geophys Res, 2007, 34, L17603, doi: 10.1029/2007GL030410.

[10] LIU Zheng-qi, LIU Yu-guo, HA Yao, et al. Role of equatorial Pacific Ocean subsurface oceanic temperature mode in ENSO cycle [J]. J Trop Meteorol, 2014, 20 (4): 334-341.

[11] KHAIN A P, GINIS I. The mutual response of a moving tropical cyclone and the ocean [J]. Beitr Phys Atmos, 1991, 64(1): 125-142.

[12] YUAN J P, JIANG J. The relationships between tropical cyclone tracks and local SST over the western North Pacific [J]. J Trop Meteorol, 2011, 17(2): 120-127.

[13] ZHANG Zhong-feng, LIU Qi-han, TUO Rrui-fang. Numerical study of the abnormal track of Typhoon Maggie [J]. J Trop Meteorol, 2006, 12(2): 174-178.

[14] BENDER M A, GINIS I. Real-case simulations of hurricane-ocean interaction using high-resolu tion coupled model: Effects on hurricane intensity [J]. Mon Wea Rev, 2000, 128: 917-946.

[15] ZHU H Y, ULRICH W, SMITH R. Ocean effects on tropical cyclone intensification and inner-core asymmetries [J]. J Atmos Sci, 2004, 61: 1 245-1 258.

[16] WU L, WANG B, BRAUN S A. Impacts of air-sea interaction on tropical cyclone track and intensity [J]. Mon Wea Rev, 2005, 133, 3 299-3 314. dio: 10.1175/MWR3030.1

[17] RICHARD W R, SMITH T M, LIU C Y, et al. Daily High-Resolution Blended Analyses for Sea Surface Temperature [EB/OL]. 2007. ftp://eclipse.ncdc.noaa.gov/pub/OI-daily/ daily-sst.pdf

[18] BLANC F C, SCHGOUNN et al. Merged Topex/Poseidon Products [EB/OL].1996. http://www.aviso.oceanobs.com

[19] SHIE C L. Reprocessing and Goddard Satellite-based Surface Turbulent Fluxes (GSSTF) Data Set for Global Water and Energy Cycle Research [EB/OL]. 2009. http://www.ncdc.noaa.gov/sites/default/files/attachments/Reynolds2009_oisst_daily_v02r00_version2-features.pdf

[20] HWANG C, WU C R, KAO R. TOPEX/Poseidon observations of mesoscale eddies over the subtropical countercurrent: kinematic characteristics of all anticyclonic eddies and of a cyclonic eddy [J]. J Geophy Res, 2004, 109 (17): 1-17.

[21] ANTHES R A, CHANG S W. Response of the hurricane boundary layer to changes of sea surface temperature in a

numerical model [J]. J Atmos Sci, 1978, 35(1): 1 240-1 255.
[22] LIU Xiang, JIANG Guo-rong, ZHUO Hai-feng. Numerical experiment for the impact of SST to typhoon "Chanchu" [J]. Mar Fore, 2009, 3(1): 1-11.
[23] XU Ying-long, ZHANG Ling, GAO Shuan-zhu. The advances and discussions on China peroration typhoon forecasting [J]. Meteorol Mon, 2010, 36(3): 43-49.
[24] WU L, WANG B. Effects of convective heating on movement and vertical coupling of tropical cyclones: a numerical study [J]. J Atmos Sci, 2001, 58(1): 3 639-3 649.
[25] CHEN Zi-tong. A possible reason of track variation of Vongfong during landing [J]. J Trop Meteorol, 2004, 20 (6): 625-633(in Chinese).

Citation: LAI Qiao-zhen, WU Li-guang and SHIE Chung-lin. Sea surface temperature response to typhoon Morakot (2009) and its influence [J]. J Trop Meteorol, 2015, 21(2): 111-120.